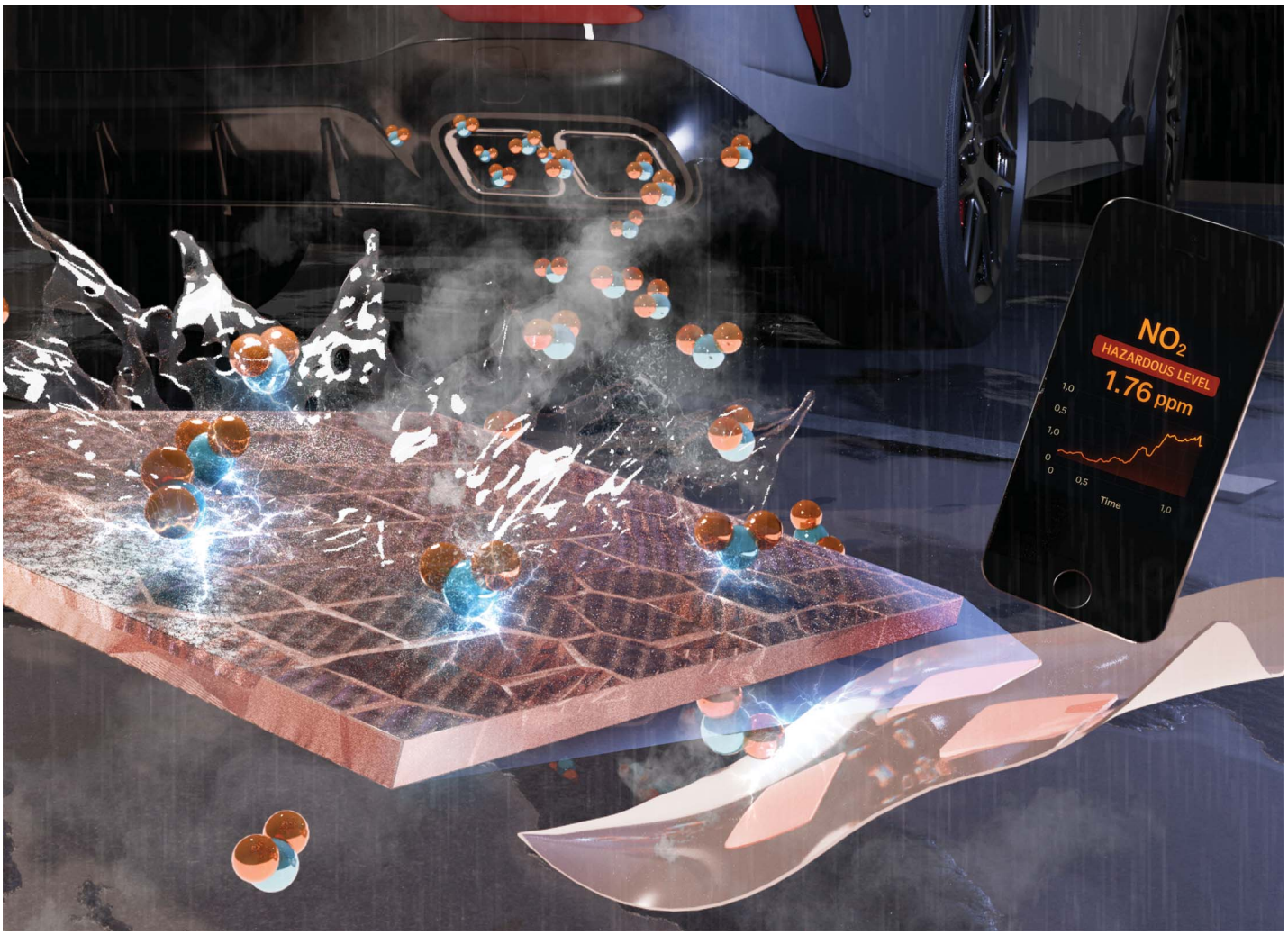

Showcasing research from Professor Junwoo Lee's laboratory, Department of Molecular Science and Technology, Ajou University, Suwon 16499, Republic of Korea.

Enhancing NO_2 sensing performance and stability: low-crystallinity conjugated polymers with localized aggregates *via* ethylene glycol pendants

Conjugated polymers are vital for detecting harmful gases, but balancing gas diffusion and crystallinity is challenging. We demonstrate an ethylene glycol-based low crystallinity design that enhances NO_2 sensing and stability.

Image reproduced by permission of Ji-Soo Jang and Junwoo Lee from *J. Mater. Chem. A*, 2025, **13**, 11323.

As featured in:

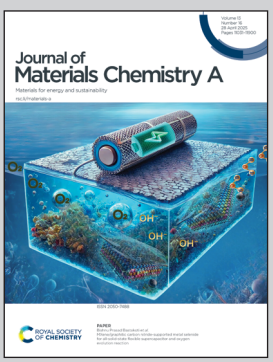

See Ji-Soo Jang, Junwoo Lee *et al.*, *J. Mater. Chem. A*, 2025, **13**, 11323.

ROYAL SOCIETY OF CHEMISTRY

rsc.li/materials-a

Registered charity number: 207890

Journal of Materials Chemistry A

ROYAL SOCIETY OF CHEMISTRY

PAPER

View Article Online
View Journal | View Issue

Cite this: J. Mater. Chem. A, 2025, 13, 11323

Enhancing NO_2 sensing performance and stability: low-crystallinity conjugated polymers with localized aggregates *via* ethylene glycol pendants†

Jung-Won An, [ab] Ho Won Jang, [bc] Ji-Soo Jang *[ad] and Junwoo Lee *[e]

Received 14th February 2025
Accepted 18th March 2025

DOI: 10.1039/d5ta01220a

rsc.li/materials-a

Conjugated polymers are of utmost importance for the detection of harmful gas phase chemicals. However, the development of highly sensitive polymers remains a challenge due to the trade-off between gas diffusion and crystallinity. In this study, we report a solution to this issue based on low crystallinity with localized aggregates. This designed morphology mediated by substitution with ethylene glycol pendant groups not only enhances electrical conductivity but also simultaneously improves the diffusion and affinity between the polymer matrix and nitrogen dioxide. Moreover, the promoted amorphous nature suppressed morphological degradation, thus offering highly sensitive chemiresistors with enhanced stability against elevated temperature.

1. Introduction

Urbanization and industrialization markedly enhance the convenience of human existence while concurrently exerting substantial disruption on the ecological environment. Nitrogen dioxide (NO_2), particularly produced through the combustion of fossil fuels, poses significant threats to both the environment and human health.[1,2] The NO_2 gas can engage in photochemical reactions with other contaminants or water, leading to the formation of ozone or acid rain, amplifying its detrimental impact on the environment.[3,4] Furthermore, at extremely low concentrations (<10 ppm), the gas can lead to symptoms like nose and throat discomfort, temporary coughing, eye irritation, fatigue, and nausea.[5,6] In this regard, developing highly sensitive NO_2 sensing devices has become one of the most important techniques.

Chemiresistors, composed of active layers and electrodes, have gained significant interest as sensor devices due to their minimalist architecture, which offers advantages in mass production and cost compared to field effect transistors (FETs) and optical sensors.[7–10] Sensitivity of chemiresistors is generated by leveraging transduction based on resistance changes resulting from the interaction with a specific chemical in active layers.[11] In the selection of active materials, metal oxides can enable detection of NO_2 through chemical interactions with oxygen ions adsorbed on the metal oxide.[12] However, these sensor devices typically operate at elevated temperatures, making it a primary objective to bring their operating temperature down to ambient levels.[13] Conversely, two-dimensional (2D) materials such as silicon arsenide, molybdenum disulfide or graphene can be utilized to fabricate sensor devices that operate at room temperature.[14–16] However, their functionality mainly hinges on the charge transfer between the active layers and the physically adsorbed gas molecules. As a result, they are responsive to a broad range of dipolar gases, indicating limited selectivity to NO_2.

Conjugated polymers (CPs) have emerged as promising candidates to detect NO_2 under ambient conditions, owing to

[a]Electronic and Hybrid Materials Research Center, Korea Institute of Science and Technology, Seoul 02792, Republic of Korea. E-mail: wkdwltn92@kist.re.kr
[b]Department of Materials Science and Engineering, Research Institute of Advanced Materials, Seoul National University, Seoul 08826, Republic of Korea
[c]Advanced Institute of Convergence Technology, Seoul National University, Suwon 16229, Republic of Korea
[d]Division of Energy and Environment Technology, KIST School, University of Science and Technology, Seoul 02792, Republic of Korea
[e]Department of Molecular Science and Technology, Ajou University, Suwon 16499, Republic of Korea. E-mail: junwoolee@ajou.ac.kr

† Electronic supplementary information (ESI) available. See DOI: https://doi.org/10.1039/d5ta01220a

Junwoo Lee

Junwoo Lee is an Assistant Professor in the Department of Molecular Science and Technology at Ajou University in South Korea. He earned his PhD in Chemical Engineering from the Pohang University of Science and Technology (POSTECH) in 2020. Following his doctoral studies, he worked as a postdoctoral researcher in the Department of Chemical and Environmental Engineering at Yale University in the United States. His current research focuses on the synthesis of functional polymeric materials.

selective interaction between specific moieties in CPs and target gas molecules.[17] Through this interaction, CPs readily transfer electrons to NO_2 gas, resulting in significant resistance changes. For example, imine units are weakened *via* interaction with NO_2. This facilitates the disconnection of π-conjugation and a subsequent increase in resistance.[18] Pyrrole and thiophene units can be doped, where π-electrons in the units react with NO_2.[19,20] This modulates the charge density and mobility, diminishing the resistance of the semiconducting CPs to a highly conductive state.[21] However, the CPs are inevitably limited to semicrystalline morphology resulting from a highly ordered molecular structure.[22] Given that gaseous NO_2 molecules exhibit limited immobilization capabilities owing to their rigorous molecular dynamics, the polymer morphology becomes a critical factor for the diffusion of NO_2 into the polymer matrix.[23] Highly crystalline CPs, in fact, have shown to be unsuitable for sensitive chemiresistors due to their limited diffusion in the crystalline region.[24] This restricted diffusion not only reduces the affinity between CPs and NO_2 but also ultimately diminishes the sensitivity of chemiresistors.[25] Taken together, optimizing polymer morphology to enhance sensitivity remains underexplored.

Herein, we present a facile approach to improving the sensitivity of NO_2 chemiresistors based on ethylene glycol pendant groups. This approach simultaneously facilitates charge mobility and NO_2 diffusion through low-crystallinity CPs with localized aggregates. In our design, triethylene glycol (TEG) pendant groups were introduced into CPs based on benzothiadiazole, thienothiophene, and NO_2 sensitive thiophene units (PTEGTT) (Fig. 1a). We hypothesize that the substitution of TEG pendant groups promotes amorphous nature and π–π stacking simultaneously due to their flexibility. This promotes the formation of localized aggregates, enhancing electrical conductivity related to charge mobility by π-orbital overlap among multiple conjugated backbones within amorphous regions.[26] The resulting low crystallinity increases unoccupied space between electronic clouds of polymer chains, referred to as free volume.[27] The gas molecules occupy the free volume, facilitating the diffusion of NO_2 into the CP matrix.[28] Furthermore, the polarity of TEG groups not only can result in enhancement in the affinity between the CP and NO_2 for improving sensitivity but also can further amplify the sensitivity under humid conditions due to their hygroscopicity.[29] In addition to sensitivity enhancements, the low crystallinity resulting from TEG groups was found to be critical to thermal stability, suppressing morphological degradation related to lateral crystallization against heat.[30] Highly sensitive and thermally stable NO_2 chemiresistors were fabricated from PTEGTT, demonstrating NO_2 sensitivity 3 times higher than that of the common alkyl-substituted CP (PC8TT).

2. Results and discussion

2.1. Molecular characterization of CPs

The polymers were prepared *via* the Stille coupling reaction at 110 °C in toluene (Scheme S1†). The chemical structures were confirmed using $^1H/^{13}C$ nuclear magnetic resonance (NMR) spectroscopy (Fig. S1†). In the GPC profiles with chlorobenzene as the eluent at 40 °C and polystyrene as the calibration standard, PC8TT and PTEGTT showed a number-average molecular weight (M_n) of 8.05 kDa and 7.97 kDa with dispersity ($Đ$) of 2.64 and 2.41, respectively (Fig. S2†). To investigate the thermal degradation, thermogravimetric analysis (TGA) was conducted (Fig. S3†). Both polymers showed a degradation temperature (T_d) of approximately 350 °C, indicating sufficiently high degradation temperature for relevant applications against thermal degradation.

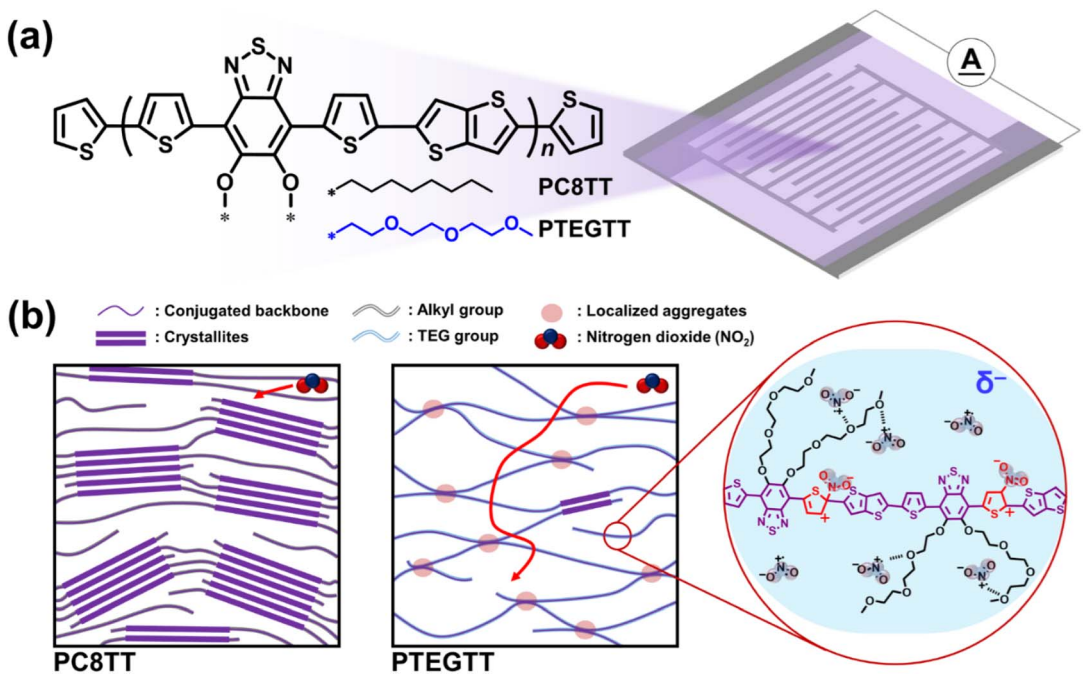

Fig. 1 (a) Chemical structure of the CPs for chemiresistors. (b) Schematic illustrations of the polymer morphologies and NO_2 behavior in the CPs.

2.2. Effect of ethylene glycol pendant groups on electrical conductivity

The influence of pendant groups on molecular packing and energy level configuration can be estimated by characterizing spectroscopic and electrochemical properties. Both polymer thin films displayed distinct absorptions at 340 nm, 430 nm, and 570 nm in UV-vis spectroscopy (Fig. 2a). The absorptions at 340 nm and 430 nm are ascribed to π–π* excitation in the thiophene and thienothiophene moieties, while the absorption at 570 nm is indicative of intramolecular charge transfer (ICT) from the donor to acceptor.[31] The degree of coplanarity of the films can be determined from the proportion of intensity between the π–π* excitation and ICT peaks.[32] The PTEGTT film exhibited a larger difference in the proportion, indicating enhanced coplanarity compared to the PC8TT film. Regarding intermolecular interactions associated with π–π stacking, the PTEGTT film not only exhibited an amplified ICT shoulder peak centered at 605 nm, denoting enhanced intermolecular aggregation, but also manifested a red-shifted ICT peak, signifying closer π–π stacking with extended conjugation length.[33,34] For electrochemical characterization, cyclic voltammetry (CV) was conducted to determine the energy level configurations. The highest occupied molecular orbital (HOMO) levels of PC8TT and PTEGTT were calculated to be −5.11 eV and −4.84 eV, obtained from the onsets of oxidation at 0.82 V and 0.55 V, respectively (Fig. 2b). To determine the lowest unoccupied molecular orbital (LUMO) levels, the optical band gap energies were calculated from the absorption onset.[35] The lowest unoccupied molecular orbital (LUMO) levels of PC8TT and PTEGTT were determined to be −3.33 eV and −3.10 eV. The difference in energy levels is attributed to the extended conjugation length arising from the flexible TEG pendant groups in PTEGTT. The spectroscopic and electrochemical properties were reflected in improved electrical conductivity (σ). The PTEGTT film exhibited a higher σ of 8.82 cS m^{-1} than that of the PC8TT film (1.31 cS m^{-1}) in a direct current circuit (Fig. 2c).

2.3. Low-crystallinity with localized aggregates

To examine the microstructure and crystallinity, we conducted two-dimensional grazing-incidence wide-angle X-ray scattering (2D-GIWAXS) measurements (Fig. 3a–c). The linear alkyl pendant groups in PC8TT favorably contributed to lamellar inter-chain packing, resulting in strong lamellar crystallite peaks (α00) with an edge-on orientation.[36] In contrast, PTEGTT exhibited a notable reduction in lamellar crystallite peaks and enhanced π–π stacking peaks (0β0) with a face-on orientation. The quantitative study on the microstructure was conducted by differential scanning calorimetry (DSC). PC8TT exhibited an endothermic transition associated with the melting of crystallites associated with the octyl pendant group (3.14 J g^{-1}), whereas PTEGTT displayed no such transition (Fig. 3d).[37] Interestingly, PTEGTT exhibited a notable exothermic transition (34.42 J g^{-1}) related to conjugated backbone packing, which was significantly more pronounced than that seen in PC8TT (9.56 J g−1). Furthermore, we calculated the distances of π–π stacking (0β0) to be 3.36 Å and 3.22 Å in PC8TT and PTEGTT (Fig. S4†). Overall, the flexibility of the TEG group in PTEGTT facilitates low-crystallinity with localized aggregates, promoting closer π–π stacking.

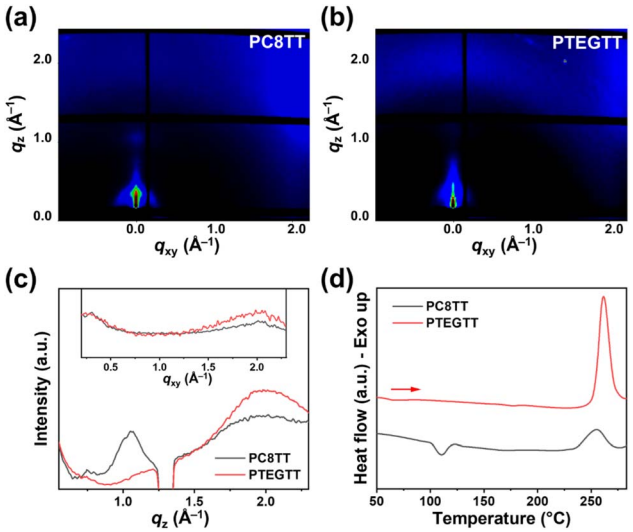

Fig. 3 2D-GIWAXS images of (a) PC8TT and (b) PTEGTT and (c) X-ray diffraction spectra extracted from the 2D-GIWAXS data. (d) DSC profiles of the polymers.

2.4. Polarity

Hansen solubility parameters (HSPs) were employed to quantitatively assess the polarity dependence on the chemical

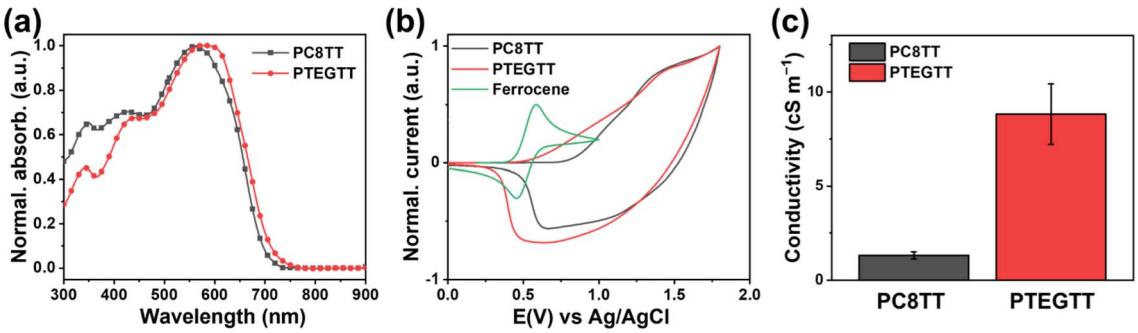

Fig. 2 (a) UV-vis spectra, (b) cyclic voltammogram, and (c) electrical conductivity (σ) of PC8TT and PTEGTT in film state.

structure. HSPs, encompassing cohesive energy densities of dispersion (δ_D), polar interaction (δ_P), and hydrogen bonding (δ_H) and interaction radius (R_0), were empirically determined based on the state of dissolution in various solvents (Fig. 4a).[38,39] The calculated HSP values for PC8TT were $\delta_D = 17.9$, $\delta_P = 4.4$, $\delta_H = 5.0$ MPa$^{0.5}$, and $R_0 = 4.5$; and for PTEGTT, they were $\delta_D = 18.2$, $\delta_P = 4.9$, $\delta_H = 5.3$ MPa$^{0.5}$, and $R_0 = 4.2$. The higher δ_P and δ_H values observed in PTEGTT suggest that the TEG pendant groups contribute to stronger polarity and hydrogen bonding.[40–42] This result is in good agreement with the surface energies calculated from contact angle measurements using water and glycerol (Fig. 4b). According to the Owens–Wendt–Rabel–Kaelble (OWRK) model, the surface energy of PTEGTT was 31.5 mJ m^{-2}, which is 5.6 mJ m^{-2} higher than that of PC8TT.[43]

2.5. NO_2 sensing properties

The ethylene glycol pendant groups in CPs can be introduced to improve NO_2 diffusion and affinity, providing a way to fabricate high performing chemiresistor-based sensors. A series of polymers were dissolved in 2-methylanisole as a green solvent, and the resulting polymer films were cast on the respective platinum interdigitated electrode to fabricate the chemiresistors.

The sensitivity of PC8TT and PTEGTT was evaluated at 25 °C and 40% relative humidity (RH) for six different NO_2 concentrations: 0.1, 0.5, 1, 2, 3, and 5 ppm relative to ambient air. The dynamic resistance changes were measured and converted into sensitivity, *i.e.*, $\Delta R/R_b = =(R_b - R_g)/R_b \times 100$ (%), where R_b and R_g represent the resistance in baseline gas (air) and target gas, respectively. While PC8TT showed a modest sensitivity to NO_2 ($\Delta R/R_b = 3.3\%$ at 0.1 ppm), PTEGTT exhibited a dramatically improved sensitivity ($\Delta R/R_b = 9.3\%$ at 0.1 ppm), presenting a corresponding decrease in resistance subsequent to NO_2 exposure (Fig. 5a). PTEGTT exhibited superior sensing performance compared to previously reported CP-based NO_2 sensors operating at room temperature, particularly in achieving a lower detection limit and higher sensitivity at low NO_2 concentrations (Table S1†). In addition, PTEGTT showed superior reversibility at 5 ppm of NO_2 even with a higher change of resistance than PC8TT, exhibiting a balanced strength of interaction for rapid desorption (Fig. 5b). The selectivity of PTEGTT was evaluated by examining its sensitivity towards other interfering analytes at a concentration of 5 ppm (Fig. 5c). PTEGTT solely displayed outstanding sensitivity to NO_2, thereby indicating excellent selectivity ($S_{NO_2}/S_{inter} > 2.41$, where S_{NO_2} and S_{inter} represent the

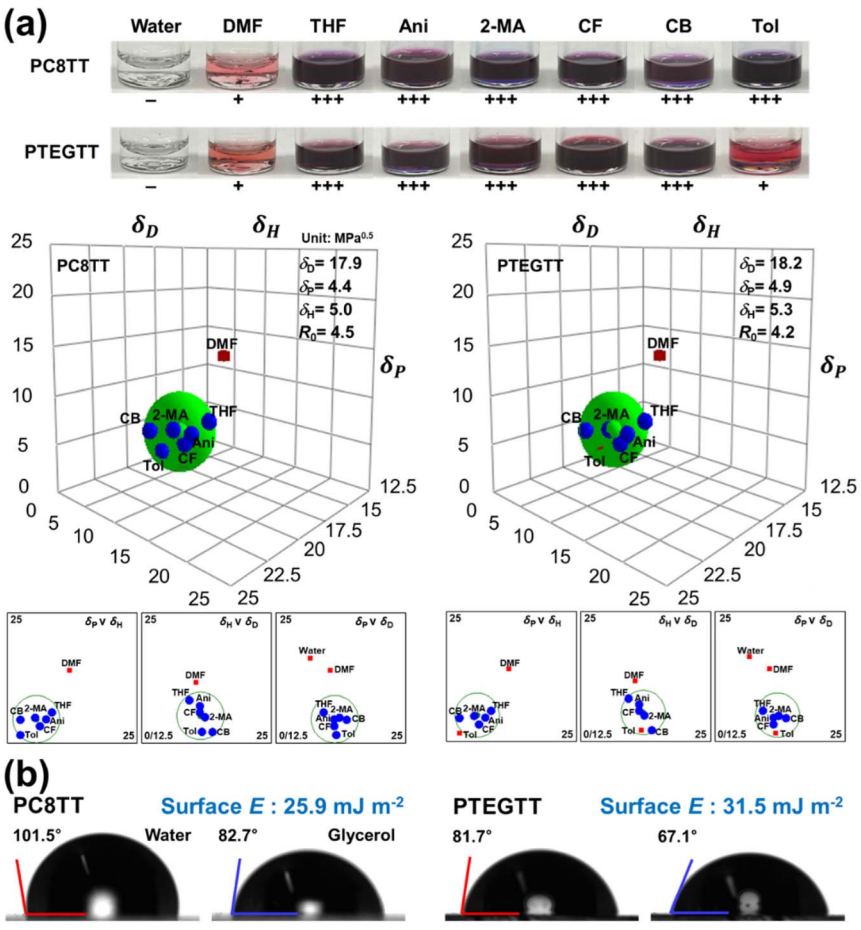

Fig. 4 (a) State of dissolution in various solvents (dimethylformamide (DMF), anisole (Ani), tetrahydrofuran (THF), chlorobenzene (CB), chloroform (CF), 2-methylanisole (2-MA), toluene (Tol)) and HSPs of PC8TT and PTEGTT, respectively. (b) Contact angles with water and glycerol and the resulting surface energies of the polymers.

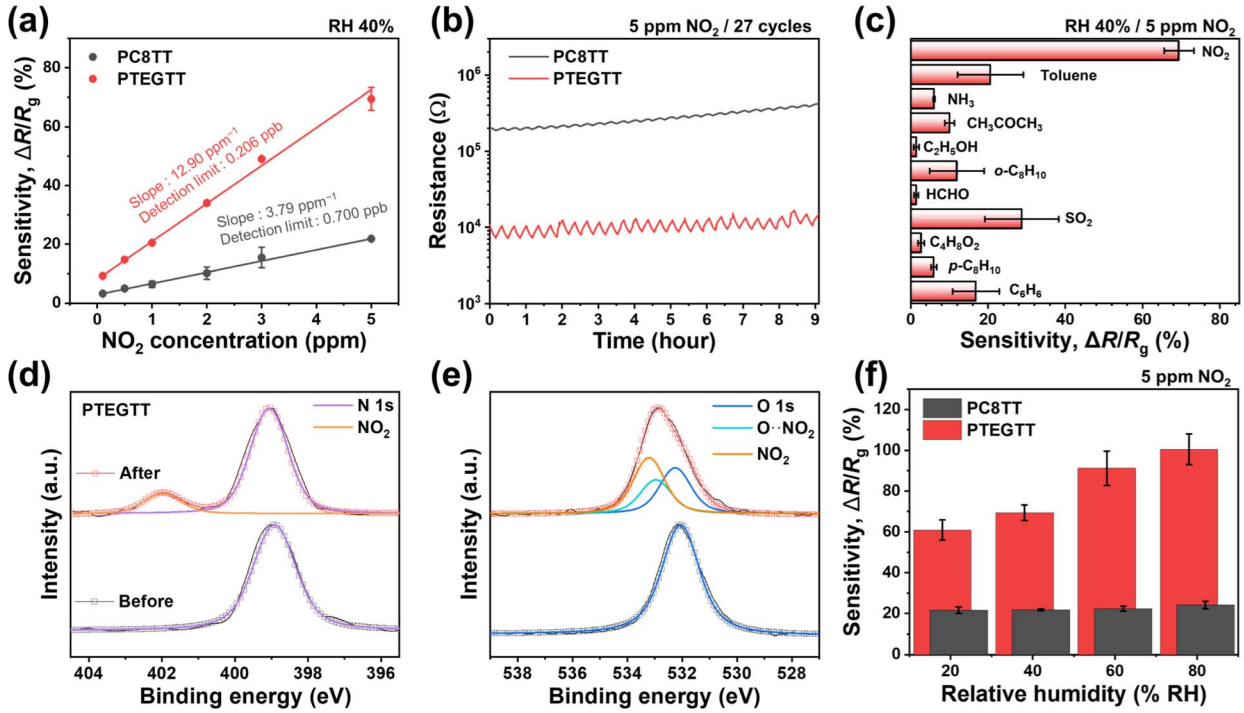

Fig. 5 NO_2 chemiresistors. (a) Sensitivity upon exposure to 0.1–5 ppm NO_2 using the CPs. (b) Resistance changes under cycling NO_2 exposure. (c) Selective sensing properties towards various analytes. XPS profiles of PTEGTT: (d) N 1s and (e) O 1s. (f) Sensitivity depending on relative humidity (RH).

sensitivity to NO_2 and interfering analytes) due to the synergistic interaction between sufficient π-electron conjugated polymers and strong oxidizing nature of NO_2.[44] To verify the NO_2 sensing ability, X-ray photoelectron spectroscopy (XPS) analysis of PC8TT and PTEGTT, targeting the 1s of nitrogen, 2s of sulfur, and 1s of oxygen, was performed after exposure to NO_2. The nitrogen XPS spectrum of PTEGTT clearly showed a peak in the presence of NO_2 (~402.0 eV) compared to PC8TT, indicating that the ethylene glycol pendant group enhanced the absorption of NO_2 by polymer films (Fig. 5d and S5†).[45] The sulfur element in PTEGTT was fitted to a doublet peak, and the additional doublet at 0.7 eV higher binding energy was assigned to the signal of the polaron formed through doping, where π-electrons in the conjugated backbone react with NO_2 (Fig. S6†).[46] Moreover, we observed the oxygen peak, indicating the interaction between TEG groups and NO_2 at 0.6 eV higher binding energy than that of pristine TEG groups (~532.2 eV) (Fig. 5e). This reflects an enhancement in absorptivity between the CP and NO_2.[47,48] These results are further supported by Fourier-transform infrared spectroscopy (FTIR) experiments conducted in the presence of NO_2 (Fig. S7†). The absorption peak corresponding to the stretching vibration of the N=O bond in NO_2 is observed at 1637 cm^{-1}.[49] Moreover, a comparative analysis between PC8TT and PTEGTT reveals that PTEGTT exhibits a significantly higher absorption intensity than PC8TT, demonstrating superior NO_2 absorption capability, attributed to the enhanced free volume and increased chemical affinity with NO_2. Additionally, the chemiresistor was subjected to an environment from 20% to 80% RH and 5 ppm of NO_2, revealing a substantial increase in NO_2 sensitivity in PTEGTT as the RH level increased ($\Delta R/R_b$ = 60.9% → 100.4%) in contrast to PC8TT ($\Delta R/R_b$ = 21.7% → 24.2%) (Fig. 5f and S8†). In FTIR, a discernible peak (~3500 cm^{-1}), indicative of O–H stretching, was exclusively observed in PTEGTT, signifying humidity absorption (Fig. S9 and S10†).[50] Consequently, the heightened sensitivities corresponding to % RH can be ascribed to these two aspects. With regard to polarity, absorbed humidity in the TEG group can lead to a greater increase in polarity, as predicted by HSP parameters (water: δ_D = 15.5 $MPa^{0.5}$, δ_P = 16.0 $MPa^{0.5}$, and δ_H = 42.3 $MPa^{0.5}$).[51] From a doping perspective, the absorbed humidity can react with NO_2, creating an acidic environment conducive to acidic doping in the conjugated backbone, thereby increasing σ.[52]

2.6. Thermal stability

The ethylene glycol pendant groups in CPs led to outstanding thermal stability. PTEGTT exhibited a greater sensitivity enhancement at 100 °C ($\Delta R/R_b$ = 20.5% → 72.0% at 1 ppm, RH 40%) than that of PC8TT ($\Delta R/R_b$ = 6.5% → 26.0%) (Fig. 6a and S11†). The enhanced sensitivity at elevated temperatures is attributed to the hopping of charge carriers within CPs according to the Schaefer–Siebert–Roth model.[53,54] In-plane X-ray scattering upon thermal aging (at 100 °C for 3 h) revealed that PC8TT exhibited an increased peak intensity associated with lateral crystallization after thermal aging, but PTEGTT displayed no changes in peak intensity (Fig. 6b). Correspondingly, atomic force microscopy (AFM) imaging revealed a considerable increase in surface roughness (RMS) in PC8TT

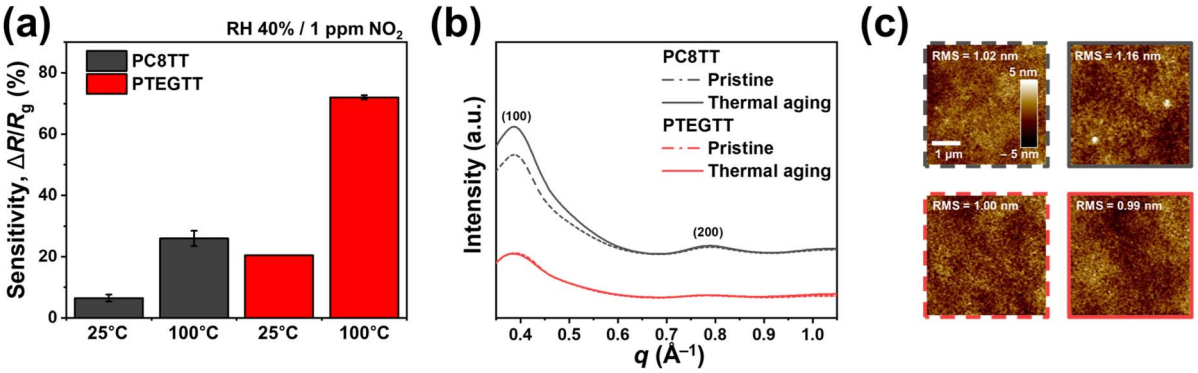

Fig. 6 (a) Sensitivity depending on temperature. (b) In-plane X-ray scattering profiles and (c) film roughness before (dashed line) and after (solid line) thermal aging.

compared to PTEGTT, increasing resistance (Fig. 6c and S12†).[55] These findings suggest that unlike in crystalline CPs, the amorphous nature of PTEGTT avoids additional crystallite formation at elevated temperatures. As a result, free volume and charge-transport pathways remain intact, preventing conductivity loss and instead leveraging thermally promoted charge-carrier hopping to enhance sensitivity.

3. Conclusions

This study demonstrated the feasibility of synthesizing highly NO_2 sensitive CPs through low crystallinity with localized aggregates *via* substitution with ethylene glycol pendant groups. The ethylene glycol-substituted PTEGTT exhibited a remarkable enhancement in amorphous nature and polarity with superior charge mobility. These improved properties led to exceptional NO_2 sensitivity in chemiresistors, driven by the increased free volume for NO_2 diffusion and heightened polarity for NO_2 affinity. Notably, the sensors retained their performance even at elevated temperatures, without morphological degradation, due to the amorphous nature. We anticipate that our approach can be a viable strategy for the development of localized aggregates in low-crystalline CPs, with potential applications in sensing devices and organic electronics.

Data availability

The authors confirm that the data supporting the findings of this study are available within the article and ESI.†

Conflicts of interest

There are no conflicts to declare.

Acknowledgements

This work was supported by the National Research Foundation of Korea (NRF), funded by the Korean government (MSIT) (RS-2024-00333848 & RS-2025-00553616), and by KIST (2E33811 & 2V10570).

References

1 S. Wu, B. Huang, J. Wang, L. He, Z. Wang, Z. Yan, X. Lao, F. Zhang, R. Liu and Z. Du, *Environ. Pollut.*, 2021, **273**, 116456.
2 S. C. Anenberg, J. Miller, R. Minjares, L. Du, D. K. Henze, F. Lacey, C. S. Malley, L. Emberson, V. Franco and Z. Klimont, *Nature*, 2017, **545**, 467–471.
3 G. Villena, I. Bejan, R. Kurtenbach, P. Wiesen and J. Kleffmann, *Atmos. Meas. Tech.*, 2012, **5**, 149–159.
4 H. Mohajan, *Open Sci. J. Anal. Chem.*, 2018, **3**, 47–55.
5 O. Oguntoke and A. Adeyemi, *Indoor Built Environ.*, 2017, **26**, 538–550.
6 Z. Zhang, J. Wang and W. Lu, *Environ. Sci. Pollut. Res.*, 2018, **25**, 15133–15145.
7 M. S. Yao, W. X. Tang, G. E. Wang, B. Nath and G. Xu, *Adv. Mater.*, 2016, **28**, 5229–5234.
8 L. Albero Blanquer, F. Marchini, J. R. Seitz, N. Daher, F. Bétermier, J. Huang, C. Gervillié and J.-M. Tarascon, *Nat. Commun.*, 2022, **13**, 1153.
9 E. J. Choi, N. P. Drago, N. J. Humphrey, J. Van Houten, J. Ahn, J. Lee, I.-D. Kim, A. F. Ogata and R. M. Penner, *Mater. Today*, 2022, **62**, 129–150.
10 E. Piccinini, G. E. Fenoy, A. L. Cantillo, J. A. Allegretto, J. Scotto, J. M. Piccinini, W. A. Marmisollé and O. Azzaroni, *Adv. Mater. Interfaces*, 2022, **9**, 2102526.
11 J. G. Weis, J. B. Ravnsbæk, K. A. Mirica and T. M. Swager, *ACS Sens.*, 2016, **1**, 115–119.
12 Y. Cheng, B. Ren, K. Xu, I. Jeerapan, H. Chen, Z. Li and J. Z. Ou, *J. Mater. Chem. C*, 2021, **9**, 3026–3051.
13 W. Shin, S. Hong, Y. Jeong, G. Jung, J. Park, D. Kim, C. Lee, B.-G. Park and J.-H. Lee, *Nanoscale*, 2021, **13**, 9009–9017.
14 S. W. Lee, W. Lee, Y. Hong, G. Lee and D. S. Yoon, *Sens. Actuators, B*, 2018, **255**, 1788–1804.
15 A. V. Agrawal, N. Kumar and M. Kumar, *Nano-Micro Lett.*, 2021, **13**, 1–58.
16 J. Zhao, X. Cui, Q. Huang and H. Zeng, *Appl. Surf. Sci.*, 2023, **613**, 156010.
17 Z. Ding, D. Liu, K. Zhao and Y. Han, *Macromolecules*, 2021, **54**, 3907–3926.

18 H. Park, D. H. Kim, B. S. Ma, E. Shin, Y. Kim, T. S. Kim, F. S. Kim, I. D. Kim and B. J. Kim, *Adv. Sci.*, 2022, **9**, 2200270.
19 A. Kumar, P. Jha, A. Singh, A. Chauhan, S. Gupta, D. Aswal, K. Muthe and S. Gadkari, *Chem. Phys. Lett.*, 2018, **698**, 7–10.
20 M. Huang, Y. Wang, S. Ying, Z. Wu, W. Liu, D. Chen and C. Peng, *Sensors*, 2021, **21**, 1958.
21 Y. Yamashita, J. Tsurumi, M. Ohno, R. Fujimoto, S. Kumagai, T. Kurosawa, T. Okamoto, J. Takeya and S. Watanabe, *Nature*, 2019, **572**, 634–638.
22 H. Tanaka, A. Wakamatsu, M. Kondo, S. Kawamura, S.-i. Kuroda, Y. Shimoi, W.-T. Park, Y.-Y. Noh and T. Takenobu, *Commun. Phys.*, 2019, **2**, 96.
23 W. Huang, X. Zhuang, F. S. Melkonyan, B. Wang, L. Zeng, G. Wang, S. Han, M. J. Bedzyk, J. Yu and T. J. Marks, *Adv. Mater.*, 2017, **29**, 1701706.
24 P. Hrdlovic, J. Pavlinec and H. Jellinek, *J. Polym. Sci., Part A: Polym. Chem.*, 1971, **9**, 1235–1245.
25 D. Wang, Y. Hu, J. Zhao, L. Zeng, X. Tao and W. Chen, *J. Mater. Chem. A*, 2014, **2**, 17415–17420.
26 S. Y. Son, Y. Kim, J. Lee, G.-Y. Lee, W.-T. Park, Y.-Y. Noh, C. E. Park and T. Park, *J. Am. Chem. Soc.*, 2016, **138**, 8096–8103.
27 H. Kanesugi, K. Ohyama, H. Fujiwara and S. Nishimura, *Int. J. Hydrogen Energy*, 2023, **48**, 723–739.
28 M. Meunier, *J. Chem. Phys.*, 2005, **123**, 134906.
29 N. Kubochkin and N. Ivanova, *Langmuir*, 2019, **35**, 5054–5059.
30 J. Lee, J. W. Kim, S. A. Park, S. Y. Son, K. Choi, W. Lee, M. Kim, J. Y. Kim and T. Park, *Adv. Energy Mater.*, 2019, **9**, 1901829.
31 Y. Wang, W. Chen, L. Wang, B. Tu, T. Chen, B. Liu, K. Yang, C. W. Koh, X. Zhang and H. Sun, *Adv. Mater.*, 2019, **31**, 1902781.
32 J. Sun, Z. Liu, H. Luo, S. Yang, J. Yao, G. Zhang and D. Zhang, *J. Mater. Chem. C*, 2016, **4**, 9359–9365.
33 H. Zhang, H. Yao, W. Zhao, L. Ye and J. Hou, *Adv. Energy Mater.*, 2016, **6**, 1502177.
34 C. R. Bridges, M. J. Ford, E. M. Thomas, C. Gomez, G. C. Bazan and R. A. Segalman, *Macromolecules*, 2018, **51**, 8597–8604.
35 M. Alsufyani, M.-A. Stoeckel, X. Chen, K. Thorley, R. K. Hallani, Y. Puttisong, X. Ji, D. Meli, B. D. Paulsen, J. Strzalka, K. Regeta, C. Combe, H. Chen, J. Tian, J. Rivnay, S. Fabiano and I. McCulloch, *Angew. Chem., Int. Ed.*, 2022, **61**, e202113078.
36 M. Brinkmann and P. Rannou, *Adv. Funct. Mater.*, 2007, **17**, 101–108.
37 H. Chen, C. Su, G. Shi, G. Liu and D. Wang, *Eur. Polym. J.*, 2018, **99**, 284–288.
38 C. M. Hansen, The Three Dimensional Solubility Parameter and Solvent Diffusion Coefficient: Their Importance in Surface Coating Formulation, *PhD thesis*, Technical University of Denmark, Copenhagen, 1967.
39 J. Lee, G. W. Kim, M. Kim, S. A. Park and T. Park, *Adv. Energy Mater.*, 2020, **10**, 1902662.
40 J. Sherwood, A. Constantinou, L. Moity, C. R. McElroy, T. J. Farmer, T. Duncan, W. Raverty, A. J. Hunt and J. H. Clark, *Chem. Commun.*, 2014, **50**, 9650–9652.
41 X. Jiang, H. Gao, X. Zhang, J. Pang, Y. Li, K. Li, Y. Wu, S. Li, J. Zhu and Y. Wei, *Nat. Commun.*, 2018, **9**, 3799.
42 J. Lee, S. A. Park, S. U. Ryu, D. Chung, T. Park and S. Y. Son, *J. Mater. Chem. A*, 2020, **8**, 21455–21473.
43 H. Feng, M. Dolejsi, N. Zhu, S. Yim, W. Loo, P. Ma, C. Zhou, G. S. Craig, W. Chen and L. Wan, *Nat. Mater.*, 2022, 92–99.
44 H. Li, J. Dailey, T. Kale, K. Besar, K. Koehler and H. E. Katz, *ACS Appl. Mater. Interfaces*, 2017, **9**, 20501–20507.
45 J. Baltrusaitis, P. M. Jayaweera and V. H. Grassian, *Phys. Chem. Chem. Phys.*, 2009, **11**, 8295–8305.
46 B. Wegner, D. Lungwitz, A. E. Mansour, C. E. Tait, N. Tanaka, T. Zhai, S. Duhm, M. Forster, J. Behrends and Y. Shoji, *Adv. Sci.*, 2020, **7**, 2001322.
47 O. Rosseler, M. Sleiman, V. N. Montesinos, A. Shavorskiy, V. Keller, N. Keller, M. I. Litter, H. Bluhm, M. Salmeron and H. Destaillats, *J. Phys. Chem. Lett.*, 2013, **4**, 536–541.
48 D. N. Voylov, A. P. Holt, B. Doughty, V. Bocharova, H. M. Meyer III, S. Cheng, H. Martin, M. Dadmun, A. Kisliuk and A. P. Sokolov, *ACS Macro Lett.*, 2017, **6**, 68–72.
49 Z. Zhang, J. Chu, H. Hu, H. Sun, X. Zhao, H. Du and M. Yang, *ACS Sens.*, 2024, **9**, 4134–4142.
50 B. L. Mojet, S. D. Ebbesen and L. Lefferts, *Chem. Soc. Rev.*, 2010, **39**, 4643–4655.
51 C. Jia, S. Xie, W. Zhang, N. N. Intan, J. Sampath, J. Pfaendtner and H. Lin, *Chem Catal.*, 2021, **1**, 437–455.
52 S. Jain, S. Chakane, A. Samui, V. Krishnamurthy and S. Bhoraskar, *Sens. Actuators, B*, 2003, **96**, 124–129.
53 A. Gumyusenge, D. T. Tran, X. Luo, G. M. Pitch, Y. Zhao, K. A. Jenkins, T. J. Dunn, A. L. Ayzner, B. M. Savoie and J. Mei, *Science*, 2018, **362**, 1131–1134.
54 K. Namsheer and C. S. Rout, *RSC Adv.*, 2021, **11**, 5659–5697.
55 D. Wang and T. P. Russell, *Macromolecules*, 2018, **51**, 3–24.